



NUMERICAL INVESTIGATION FOR THE LAMINAR FLOW EFFECTS OVER ROUGH SURFACE USING DIRECTION SPLITTING

Mei Su^a, Ligai Kang^b, Kangjie Sun^{b*}

^a School of Mechanical Engineering, Lanzhou Jiaotong University, Lanzhou, 730070, China

^b School of Civil Engineering, Hebei University of Science and Technology, Shijiazhuang, Hebei, 050018, China

ABSTRACT

To study the heat transfer effect of rough surface in laminar flow, the direction splitting method is introduced by fully developed fields for solving the Navier–Stokes equations of incompressible flow in assuming two-dimension. Firstly, the algorithm of the incompressible Navier–Stokes equations with pressure correct is carried out. Secondly, the effects of pressure drop and heat transfer are investigated in different rough surface elements which are configured with triangular and rectangular elements. The Reynolds number, roughness element spacing, and roughness height are also considered as the factors which affect the heat transfer. The results indicate that the parallel present method reaches the stage of basically stable state rapidly and accurately. Compared with the smooth surface, the global performance of heat transfer is improved by the roughness surface since the pressure drop is lost. The effects of triangular element roughness surface on laminar flow and heat transfer are much stronger than rectangular element roughness surface when the spacing of the rough is changed. The flow over the triangular element roughness surface becomes stronger, which contributes to enhancement heat transfer meanwhile increase the pressure drop when the roughness height is higher.

Keywords: heat transfer, roughness surface, direction splitting

1. INTRODUCTION

Heat transfer in roughness surface is more and more important due to its many enhanced practical applications, such as industry and heat dissipation of electronic component. There are many passive enhancement heat transfer techniques used, such as cylinders, fins, and plates which named as vortex generators. The geometric factors of vortex generators play significant effects in the pressure drop and enhance heat transfer rate due to it can enhance the heat transfer. Because vortex generators can disturb the increasing fluid mixing and interrupt the development of the thermal boundary layer for enhancement of heat transfer.

Many investigators have researched enhance heat transfer by rough surface. In 1980s, Tuckerman and Pease (1981) worked on rough surface firstly. Sultan (2000) investigated that the perforated holes can induce the heat transfer enhancement by experiment. It is found that the average heat transfer coefficient increased up to 33.15% by using different area ratio of the opening hole in experiment. Ma *et al.* (2020) experimentally researched the heat transfer characteristics of water flow through rough fractures. Nilpueng *et al.* (2015) researched the effect on heat transfer coefficient and pressure drop at Reynolds numbers ranging between 1300 and 3200 inside a plate heat exchanger with different surface roughness. Habet *et al.* (2022) investigated the heat transfer and fluid flow characteristics in a rectangular channel with baffles mounted on the top and the bottom surfaces in a staggered arrangement. They found that the proposed baffles can enhance heat transfer obviously. Modi and Rathod (2022) studied the heat transfer effect of vortex generators for a fin-tube heat exchanger by experimental results. The results show that the vortex generator can heavily enhance the heat transfer.

In numerical simulation, Fu *et al.* (2012) studied heat Transfer characteristics of mixed convective heat transfer rate of a heat surface in a three-dimensional horizontal channel with insertion of a moving block. They found that the heat surface can enhanced strongly heat transfer with the moving block. Wang *et al.* (2019) investigated the influence of a series of miniature cuboid vortex generators on flow and heat transfer characteristics in a rectangular channel by CFD simulation. Sahel *et al.* (2016) found that the effect on pressure drop and heat transfer in the channel with perforated baffles having a row of four holes placed at three different positions. Compared to simple baffle, it shows that the new devices can increase the rate of heat transfer to 65%. Xiao *et al.* (2015) numerically studied the heat transfer and friction characters of different roughness elements in non-uniform wall roughness lattice. Bilen and Yapici (2002) and Bilen *et al.* (2001) studied the heat transfer of roughness surface which fitted with rectangular blocks by different angle. It shows that the angle and the Reynolds number and are the most efficient parameters in all factors. Ansari and Zhou (2020) studied the effect of roughness surface element on the pressure drop and heat transfer by finite element CFD simulation. It shows that the spacing of roughness elements which is considered for enhanced the heat transfer.

As above knowledge, how to solve Navier–Stokes equations economically and accurately is popular. Guermond and Mineev (2010) studied a method to solve the incompressible Navier–Stokes equations by using direction-splitting-based fractional time stepping. This method is very simple to program in parallel, very fast, and has exactly the same stability and convergence properties as the Poisson-based pressure-correction technique. The target of the present work is to research this method of the flow field and heat transfer effect on rough surfaces, and confirm the effects on heat transfer, pressure drop, and flow field by different geometric configurations and flow parameters using this method.

* Corresponding author. Email: sunkangjie0606@sina.com

2. HEAT TRANSFER OF ROUGH SURFACE

2.1 Mathematical Model

For analyze the heat transfer effects of roughness elements on heat transfer and pressure drop in surface, the 2D physical geometry is considered in present study as shown in Fig. 1. The three different shape surfaces roughness are investigated in present paper which include plate element, triangular element, and rectangular element. As shown in Fig. 1, it is non-dimensional assumed that h is the height of roughness element, s is the spacing that between two adjacent roughness element peaks, s_0 is the width of the single roughness elements which are all considered to be the same for rough surface on both the top and bottom surfaces, H is the height of channel, and L is the length of channel, the working fluid is air. The flow is assumed to be incompressible and steady laminar viscous Newtonian flow. At the same time, the effects of buoyancy induced are negligible. The fluid property is air and the solid property is cuprum respective. The Prandtl number of this model is equal to 0.71. It has been previously confirmed that viscous liquid flow obeys the continuum assumption on rough surface. The resulting non-dimensional equations for continuity momentum and energy equations for heat transfer in laminar flow on rough surface are as follows.

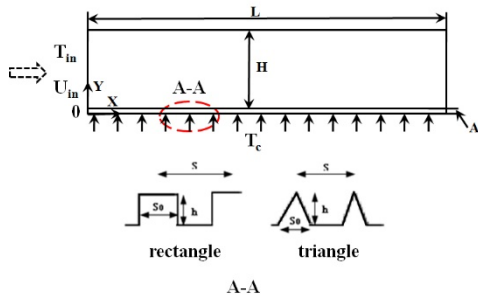


Fig. 1 Schematic of rough surface

The continuity, momentum, and energy equation for transfer in laminar flow is:

• Continuity equation:

$$\frac{\partial U}{\partial X} + \frac{\partial V}{\partial Y} = 0 \quad (1)$$

• Momentum equation:

$$\frac{\partial U}{\partial t} + U \frac{\partial U}{\partial X} + V \frac{\partial U}{\partial Y} = -\frac{\partial P}{\partial X} + \frac{1}{\text{Re}} \left(\frac{\partial^2 U}{\partial X^2} + \frac{\partial^2 U}{\partial Y^2} \right) \quad (2)$$

$$\frac{\partial V}{\partial t} + U \frac{\partial V}{\partial X} + V \frac{\partial V}{\partial Y} = -\frac{\partial P}{\partial Y} + \frac{1}{\text{Re}} \left(\frac{\partial^2 V}{\partial X^2} + \frac{\partial^2 V}{\partial Y^2} \right) \quad (3)$$

• Energy equation:

$$\frac{\partial \Theta}{\partial t} + U \frac{\partial \Theta}{\partial X} + V \frac{\partial \Theta}{\partial Y} = \frac{1}{\text{Pr} \cdot \text{Re}} \left(\frac{\partial^2 \Theta}{\partial X^2} + \frac{\partial^2 \Theta}{\partial Y^2} \right) \quad (4)$$

The non-dimensional variables of equation are defined as follow.

$$L_{\text{ref}} = H, X = \frac{x}{H}, Y = \frac{y}{H}, t_{\text{ref}} = \frac{H}{U_0}, \text{Pr} = \frac{\nu}{a}$$

$$U_r = U_0, U = \frac{u}{U_r}, V = \frac{v}{U_r}, P = \frac{p}{\rho U_r^2} \quad (5)$$

$$T_r = \min(T_{\text{in}}, T_{\text{out}}), \Theta = \frac{T - T_r}{\Delta T}, \text{Re} = \frac{U_0 H}{\nu}$$

where, L_{ref} is the characteristic length, t_{ref} is the characteristic time, u and v are the components of the velocity vector along the x , y directions respectively, p is the fluid pressure, ρ is the fluid viscosity, a is the thermal diffusivity, T is the fluid temperature, U_0 is the mean velocity of inlet flow, T_{out} is the temperature of outlet flow, T_{in} is the temperature of inlet flow.

The fluid of the inlet condition is fully developed with a parabolic profile $U_0(Y) = 6Y(1-Y)$ and the boundary conditions are:

The fluid of the inlet condition is fully developed with a parabolic profile $U_0(Y) = 6Y(1-Y)$ and the boundary conditions are:

$$X = 0, 0 \leq Y \leq A, U = 0, V = 0, \frac{\partial \Theta}{\partial X} = 0 \quad (6)$$

$$X = 0, A \leq Y \leq H, U = 1, V = 0, \Theta = 0$$

Where $U=1$ means the maximum velocity in the channel model. Meanwhile, the outlet channel can be defined as fully developed flow, and the boundary condition of outlet can be defined as:

$$X = L, 0 \leq Y \leq A, U = 0, V = 0, \frac{\partial \Theta}{\partial X} = 0 \quad (7)$$

$$X = L, A \leq Y \leq H, \frac{\partial U}{\partial X} = 0, \frac{\partial V}{\partial Y} = 0, \frac{\partial \Theta}{\partial X} = 0$$

The boundary conditions of wall and slipping condition can be defined as:

$$Y = 0, U = 0, V = 0, \Theta = 1 \quad (8)$$

$$Y = H, \frac{\partial U}{\partial Y} = 0, V = 0, \frac{\partial \Theta}{\partial Y} = 0 \quad (9)$$

Where $\Theta = 1$ means that Θ is the maximum temperature near the wall in channel. T_r is the minimum temperature between inlet and wall. All the dimensionless parameters of heat transfer and flow field are characterized based on the height of channel, and velocity of inlet.

The dimensionless parameters of Reynolds number should characterize as the channel height in the flow field and heat transfer. At the same time, the heat transfer of internal laminar flow characteristics are characterized as the Nusselt number. The local Nu number of the roughness surface where the wall located can be characterized by local temperature gradient as:

$$Nu_x = -\frac{1}{\Theta} \frac{\partial \Theta}{\partial n} \Big|_{\text{surface}} \quad (10)$$

Mean face Nusselt number is:

$$\bar{Nu} = \frac{1}{S_i} \int_0^{S_i} Nu_x dx \quad (11)$$

Where S_i is the face area, the Poiseuille number of laminar internal flow is characterized as:

$$Po = f \bar{Re} = \frac{1}{S_i} \int_0^{S_i} f(x) \text{Re}(x) dx \quad (12)$$

Where Re is the Reynolds number, f is the friction factor of the wall, and S_i is the face area.

2.2 Numerical method

The equations are solved by the finite difference. The second-order accuracy time discretization scheme is:

$$\frac{\partial f^{n+1}}{\partial t} = \frac{3f^{n+1} - 4f^n + f^{n-1}}{2\Delta t} + O(\Delta t^2) \quad (13)$$

$$f^{n+1} = 2f^n - f^{n-1} + O(\Delta t^2) \quad (14)$$

so all the equations can be defined that:

$$\frac{3f^{n+1} - 4f^n + f^{n-1}}{2\Delta t} + 2(V \cdot \nabla f)^n - (V \cdot \nabla f)^{n-1} = \nabla^2 f^{n+1} \quad (15)$$

which can be written as Helmholtz:

$$(C_f \nabla^2 - \lambda) f^{n+1} = S_f + O(\Delta t^2) \quad (16)$$

$$\text{where } \lambda = \frac{3}{2\Delta t} \quad S_f = \frac{-4f^n + f^{n-1}}{2\Delta t} + 2(V \cdot \nabla f)^n - (V \cdot \nabla f)^{n-1}$$

$$(1) f \text{ is } U, C_f = \text{Re}^{-1}, S_f = S_U$$

$$(2) f \text{ is } V, C_f = \text{Re}^{-1}, S_f = S_V$$

$$(3) f \text{ is } \Theta, C_f = \text{Re} \cdot \text{Pr}^{-1}, S_f = S_\Theta$$

(16) can be transformed to

$$(I - \frac{C_f}{\lambda} \nabla^2) f^{n+1} = -\frac{S_f}{\lambda} + O(\Delta t^3) \tag{17}$$

so we define $f^{n+1} = f^n + O(\Delta t)$ and (17) can transform to

$$(I - \frac{C_f}{\lambda} \frac{\partial^2}{\partial X^2})(I - \frac{C_f}{\lambda} \frac{\partial^2}{\partial Y^2}) \delta f = \bar{S}_f + O(\Delta t^3) \tag{18}$$

where $\bar{S}_f = -\frac{S_f}{\lambda} - (I - \frac{C_f}{\lambda} \nabla^2) f^n$, $\delta f = f^{n+1} - f^n$, $f = U, V, \Theta$

According to Guermond and Minev [23], the pressure correction algorithm is computed by solving a sequence of one dimensional elliptic problems in each spatial direction. The pressure correction can be defined that: $A\phi^{n+1} = -\frac{1}{\Delta t} \nabla U^{n+1}$, where ϕ is $P^{n+1} - P^n$.

3 RESULTS AND DISCUSSION

The uniform grids close to the surface is highly refined to capture the high-gradient velocity, temperature, and pressure near the boundary, as shown in Fig. 2. In order to make sure the grid independence of the simulation results, four tests grids are carried out which is different grids number. The grids of about 400*300 mesh cells are considered to be reliable enough to assure mesh independence.

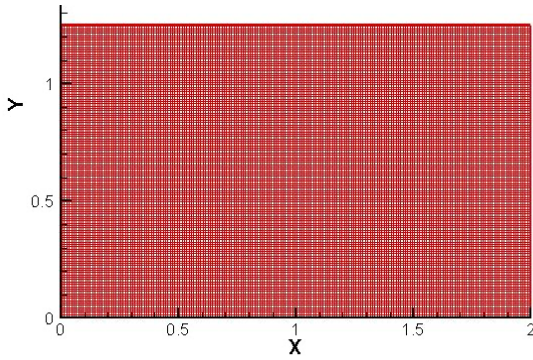


Fig. 2 Representation of the grid distribution in the channel

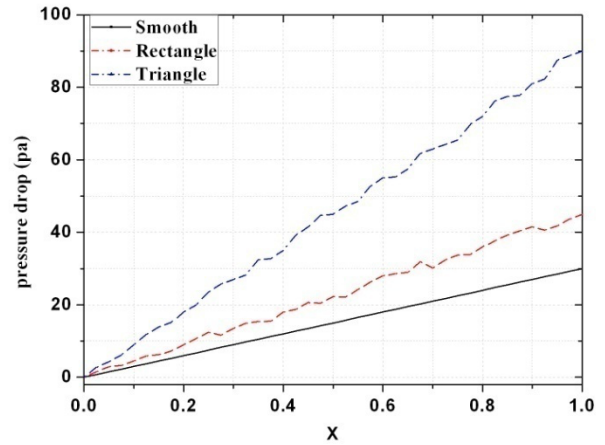
Table 1 shows that the economy of parallel version between SIMPLE and present method in different grids when Re is same. Preliminary tests show that perfect parallel scales up to the maximum number of processor that available to the authors on computer. It can clearly indicate that parallel present method is entered the stage of basically stable state rapidly. In grids of A, B and C, two methods are calculated, the operation speed of present method faster than SIMPLE because the parallel version can use CPU more reasonably. In grid of D, only new method can be run by given computer. So it can conclude that the present method is used in parallel economically when the space is regular.

Table 1 Comparison of accuracy of different schemes (Re=1000)

grids	method	Time step	Time in steady
A:200*125	SIMPLE	5e10-5	5.6sec
	Present	5e10-5	8.9sec
B:400*300	SIMPLE	2.5e10-5	12.6sec
	Present	2.5e10-5	18.6sec
C:800*600	SIMPLE	1.25e10-5	32.9 sec
	Present	1.25e10-5	66.9sec
D:1600*1200	SIMPLE	0.75e10-5	N/A
	Present	0.75e10-5	236sec

The pressure drop including smooth, rectangular, and triangular roughness elements along these local sections are given in Fig. 3. The pressure drop effect of triangular roughness elements along the channel

is higher than the rectangular roughness surface. This is the reason that the boundary layer that near the wall can regenerate and enhance the heat transfer, meanwhile, the separation and recirculation of flow is the main reason which can increase the pressure drop. The boundary layer of roughness elements can regenerate and accompany with the flow



separation generally.

Fig. 3 Local pressure drop of the local sections (Re = 1500, s=0.032, h=0.04).

Fig. 4 shows that the change of average Nusselt number and Poiseuille number with Reynolds number in rough surface. Compared with the smooth surface element, the average Poiseuille number and Nusselt number of rough surface is larger. The average Poiseuille number and Nusselt number of triangular roughness elements increase linearly with Re number.

It can conclude that the vortex effects of triangular roughness surface elements at lower Re number are much smaller than that of larger Re number. Meanwhile, the average Nu number of the rectangular element surface is decreased slightly when Re number increased, and the Po number increases slightly with Re number.

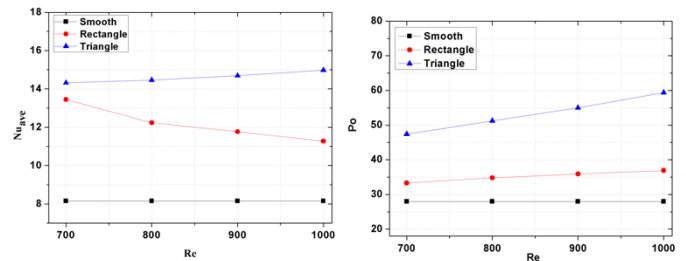


Fig.4 Effect on Re and Po with Nu (s=0.032, h=0.04).

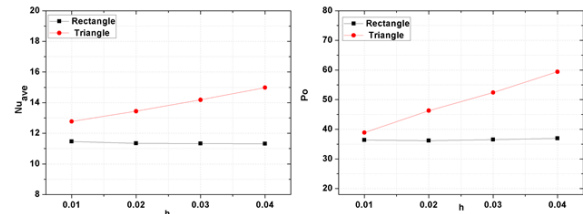


Fig.5 Effect on h on Po with Nu (Re=1000, s=0.032)

Fig. 5 shows the effect of changed roughness height on Po and Nu number. It can conclude that the average Nu numbers of triangular increases with the nearly linear when Re=1000, and the Po number also increases linearly when the roughness height increases. Meanwhile, when the height of roughness is higher, the flow of triangular roughness induces stronger recirculation and flow separation, which can influence

the thermal boundary transfer near the wall. Therefore, the temperature of fluid is resulted from heat transfer enhancement ultimately. At the same time, the pressure drop and heat transfer of rectangular roughness surface element is weaker than triangular element when the height of the roughness is changed.

Fig. 6 shows the effect of changed roughness spacing on Po number and average Nu number. It can be observed that Po and Nu are decreased as the order for rectangular and triangular roughness elements at the same spacing of the roughness elements respectively. In addition, when the spacing between the roughness elements is increased, the heat transfer is decreased for the triangular roughness element. For the rectangular roughness element, it is less significantly influenced by spacing. So it can be concluded that the heat transfer effects of triangular roughness elements are much stronger than rectangular roughness surface element in laminar flow when the spacing of the rough is changed.

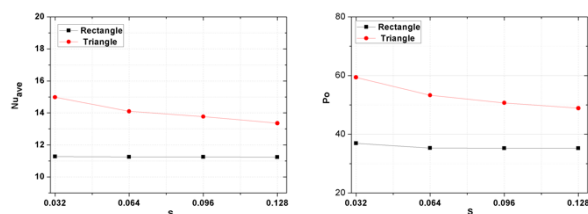


Fig.6 Effect of s on Po and Nu (Re=1000, h=0.04).

4 CONCLUSIONS

In this study, a new method with direction splitting based fractional time stepping which solves Navier–Stokes equations in different surfaces configured with smooth, rectangular, and triangular roughness elements is carried out. It can explore the effect of roughness surface elements on heat transfer with laminar flow accurately and economically. The effect of different roughness height, and roughness element spacing on heat transfer and pressure drop with different Re number in rough surfaces are investigated. The conclusions are summarized as follows:

- (1) The new method can be used in solving Navier–Stokes equations on rough surface in laminar flow more economically.
- (2) The total heat transfer of roughness surface is improved compared with the smooth surface when the pressure head is loss. Compare with the rectangular surface element, the pressure drop and local Nu number of triangular surface element is higher.
- (3) When the Re number increases, the average Po number and Nu number of rough surface are larger. The average Po number and Nu number of triangular roughness elements increase linearly with Re number.
- (4) The heat transfer effects of triangular roughness surface elements are much stronger than rectangular roughness surface element in laminar flow when the spacing of the rough is changed.
- (5) When the roughness height is higher, the flow over the triangular roughness surfaces stronger; meanwhile, the pressure drop is increased. However, the influence of the triangular surface elements element is stronger than that of rectangular surface roughness.

REFERENCES

Ansari M.Q., Zhou G.B., 2020, “Influence of Structured Surface Roughness Peaks on Flow and Heat Transfer Performances of Micro-and Mini-Channels,” *International Communications in Heat and Mass Transfer*, 110, 1028-1044.
<https://doi.org/10.1016/j.icheatmasstransfer.2019.104428>

Ansari M.Q., Zhou G.B., 2020, “Flow and Heat Transfer Analysis of Microchannels Structured with Rectangular Surface Roughness,” *Chemical Engineering and Processing - Process Intensification*, 156, 508-521.

<https://doi.org/10.1016/j.ccep.2020.108066>

Bilen K., Akyol U., 2001, “Heat Transfer and Friction Correlations and Thermal Performance Analysis for a Finned Surface,” *Energy Conversion & Management*, 42, 1071–1083.

[https://doi.org/10.1016/S0196-8904\(00\)00119-9](https://doi.org/10.1016/S0196-8904(00)00119-9)

Bilen K. and Yapici S., 2002, “Heat Transfer from a Surface Fitted with Rectangular Blocks at Different Orientation Angle,” *Heat and Mass Transfer*, 38(7–8), 649–655.

<https://doi.org/10.1007/s002310100275>

Fu W.S., Chen C.J., 2012, “Enhancement of Mixed Convection Heat Transfer in a Three-Dimensional Horizontal Channel Flow by Insertion of a Moving Block,” *International Communications in Heat and Mass Transfer*, 39, 66–71.

<https://doi.org/10.1016/j.icheatmasstransfer.2011.09.009>

Guermond J.L., Mineev P.D., 2010, “A New Class of Fractional Step Techniques for the Incompressible Navier–Stokes Equations Using Direction Splitting,” *Comptes Rendus Mathematique*, 348, 581-585.

<https://doi.org/10.1016/j.crma.2010.03.009>

Habet M.A.E., Saleh M.A., 2022, “The Effect of Using Staggered and Partially Tilted Perforated Baffles on Heat Transfer and Flow Characteristics in a Rectangular Channel,” *International Journal of Thermal Sciences*, 174, 1217-1235.

<https://doi.org/10.1016/j.ijthermalsci.2021.107422>

Ma Y.Q., Zhang Y.J., 2020, “Experimental Study of the Heat Transfer by Water in Rough Fractures and the Effect of Fracture Surface Roughness on the Heat Transfer Characteristics,” *International Journal of Heat and Mass Transfer*, 148, 1190-1207.

<https://doi.org/10.1016/j.geothermics.2019.05.009>

Modi A.J. and Rathod M.K., 2022, “Experimental Investigation of Heat Transfer Enhancement and Pressure Drop of Fin-And-Circular Tube Heat Exchangers with Modified Rectangular Winglet Vortex Generator,” *International Journal of Heat and Mass Transfer*, 189, 122-137.

<https://doi.org/10.1016/j.ijheatmasstransfer.2022.122742>

Nilpueng K., Wongwises S., 2015, “Experimental Study of Single-Phase Heat Transfer and Pressure Drop inside a Plate Heat Exchanger with a Rough Surface,” *Experimental Thermal and Fluid Science*, 68, 268-275.

<https://doi.org/10.1016/j.expthermflusci.2015.04.009>

Sultan G.I., 2000, “Enhancing Forced Convection Heat Transfer from Multiple Protruding Heat Sources Simulating Electronic Components in Horizontal Channel by Passive Cooling,” *Microelectronics Journal*, 31, 773-779.

[https://doi.org/10.1016/S0026-2692\(00\)00058-6](https://doi.org/10.1016/S0026-2692(00)00058-6)

Sahel D., Ameer H., 2016, “Enhancement of Heat Transfer in a Rectangular Channel with Perforated Baffles,” *Applied Thermal Engineering*, 101, 156-164.

<https://doi.org/10.1016/j.applthermaleng.2016.02.136>

Tuckerman B., Pease W., 1981, "High-Performance Heat Sinking for VLSI," *IEEE Electron Dev. Lett*, 126 (ELD-2).
<https://doi.org/10.1109/EDL.1981.25367>

Wang J.S., Jiao Y., 2019, "Heat Transfer and Flow Characteristics in a Rectangular Channel with Small Scale Vortex Generators," *International Journal of Heat and Mass Transfer*, 138, 208-225.

<https://doi.org/10.1016/j.ijheatmasstransfer.2019.03.138>

Xiao H.G., Chen W. Z., 2015, "Numerical Simulation of Heat Transfer and Friction in Non-Uniform Wall Roughness Lattice with Different Roughness Element Shapes," *Annals of Nuclear Energy*, 85, 732-739.
<https://doi.org/10.1016/j.anucene.2015.06.029>